ISSN 2075-1133, Inorganic Materials: Applied Research, 2019, Vol. 10, No. 4, pp. 870–874. © Pleiades Publishing, Ltd., 2019.
Russian Text © The Author(s), 2018, published in Materialovedenie, 2018, No. 11, pp. 27–31.

Elaboration of Chemical Hydrogen Source Based on Hydrides of Magnesium Alloys

I. A. Gvozdkov[a], *, V. A. Belyaev[a], S. N. Potapov[a], V. N. Verbetskii[b], S. V. Mitrokhin[b], and A. A. Tepanov[b]

[a] *OOO HeatLab, Ul'yanovsk, 432072 Russia*
[b] *Moscow State Universtiy, Moscow, 119991 Russia*
**e-mail: gvozdkov@ulnanotech.com*

Received April 26, 2018; revised June 28, 2018; accepted July 31, 2018

Abstract—In the present work, Mg–Ni–Mm alloys (where Mm is a mixture of rare earth metals) are studied to elaborate a chemical hydrogen source for portable energy systems based on fuel cells characterized by high gravimetric energy density used for unmanned air vehicles and robot systems. Hydrogen generation on demand by hydrolysis of metal hydrides (MgH_2, Mg_2NiH_4) is proposed for the fuel cell power supply because it is the most efficient method characterized by high hydrogen storage density, safety, and low costs of the stored energy. The influence of the composition of alloys on the hydrogen absorption properties and hydrogen generation during hydrolysis is studied.

Keywords: metal hydrides, hydrolysis, hydrogen absorption, magnesium hydride, magnesium alloys, hydrogen storage, fuel cells

DOI: 10.1134/S2075113319040178

INTRODUCTION

The development of the technical potential of portable devices determines the increasing demand for their power supply. The interest in hydrogen fuel cells (FC) proposed as a practical alternative to batteries is growing under these conditions. Energy systems based on hydrogen fuel cells are characterized by high specific power density which exceeds that of secondary power sources (such as lithium-ion batteries) by 3–5 times [1].

Hydrogen required for the supply of fuel cells can be stored in different forms: compressed gas, liquefied hydrogen, metals and alloys reversibly consuming hydrogen, or chemical hydrogen sources [2]. Chemical hydrogen sources such as hydrides ($NaBH_4$, NH_3BH_3, $LiAlH_4$), including metal hydrides and hydrides of intermetallic compounds (IMH) or alloys (MgH_2, CaH_2, Mg_2NiH_4), are characterized by high gravimetric hydrogen storage density. Therefore, they are promising in terms of development of high-capacity hydrogen sources.

Sodium borohydride ($NaBH_4$) is widely studied as a chemical hydrogen source among hydrides; it exhibits several advantages: explosion safety, stability in air, high hydrogen storage density (10.8 wt %), and controlled hydrogen generation [3, 4]. The publications and patents dedicated to the study of catalytic hydrolysis of sodium borohydride and description of energy systems based on this process of hydrogen generation are well known [3–9]. However, the usage of sodium borohydride is limited by the need to use a catalyst for the hydrolysis of its solution; in addition, $NaBH_4$ and the products of its hydrolysis are partially soluble in water.

Hydrolysis of hydrides of metals or alloys is another well-known method of hydrogen generation [10–12]. Thus, the specific yield of hydrogen during magnesium hydride hydrolysis is 6.4 wt % [11]. Therefore hydrogen generation by MgH_2 hydrolysis seems to be promising for mobile and portable applications. However, this method also has drawbacks. First of all, it should be mentioned that magnesium is covered by a solid layer of dihydride during hydrogenation; therefore, the hydrogenation of metal passes very slowly even under high temperatures (300–400°C).

It is advantageous to use metal powder to obtain MgH_2; however, it contains the impurity oxide phase. Moreover, the hydrolysis of magnesium dihydride is inhibited by the formation of a $Mg(OH)_2$ layer on its surface, which significantly lowers the hydrogen yield. Therefore, MgH_2 hydrolysis requires the presence of supporting substances in the solution which decompose the passivating hydroxide layer, such as metal salts [9] or organic acids [13]. Thus, it is preferable to use the hydrides characterized by a hydrogen yield comparable to MgH_2 but characterized by a higher rate

Table 1. Experimental compositions of alloys and phase components

No.	Mass fraction of components, %			Phase components
	Mg	Ni	Mm	
1	86.0	14.0	–	Mg primary + binary eutectic (Mg + Mg_2Ni)
2	74.0	26.0	–	Binary eutectic (Mg + Mg_2Ni)
3	71.0	24.0	5.0	Ternary eutectic (Mg + Mg_2Ni + $Mg_{12}Mm$)
4	66.0	26.5	7.5	Mg + Mg_2Ni + $Mg_{17}Mm_2$, Mg_2Ni primary
5	63.0	25.0	12.0	Primary Mg_2Ni + ternary eutectic
6	58.1	17.7	24.2	Eutectic (Mg_2Ni + $Mg_{17}Mm_2$)

of hydrogenation. For example, Mg_2Ni IMH exhibit a higher rate of reaction with hydrogen as compared to magnesium. In addition, the hydrides of Mg_3RE and Mg_2NiRE compounds, where RE = La, Ce, Pr, Nd [14–16], demonstrate a high rate of hydrogenation combined with high hydrogen capacity. In the present research, the hydrolysis of hydrides based on Mg–Ni–Mm alloys (where Mm is misch metal) as potentially efficient chemical hydrogen sources characterized by lower cost as compared to Mg_3RE was studied.

EXPERIMENTAL

Magnesium of the primary Mg90 grade, nickel of the primary N1 grade and, misch metal of the Mts50ZhZ grade were used as stock materials to prepare the studied samples. The compositions of alloys presented in Table 1 were selected on basis of analysis of the phase diagram of the three-component Mg–Ni–Mm system.

The samples of alloys were prepared by alloying the components in an alundum crucible in a resistance furnace. The melting was performed under cover carnallite flux of the following composition: 35 wt % KCl, 44 wt % $MgCl_2$, <1.9 wt % MgO. The melt was poured into steel molds to obtain rods with diameter and length of 15 and 120 mm, respectively. The melt stream was blown with argon to prevent oxidation.

Metallographic sections were prepared from the samples which had been cut off from the bars to study the microstructure of alloys. The sections were prepared using a Polilab P12M buffing and grinding machine; microstructure analysis was performed on a Lomo METAM LV-42 optical metallographic microscope equipped with a Nexsys Image Expert Pro image analyzer.

The study of interaction between samples and hydrogen at 330–350°C and 40 atm was performed using the facility schematically presented in Fig. 1. A more detailed description of the facility is given in [17].

The sample preliminarily purified from the oxide film and degreased using organic solvents was mechanically disintegrated and placed into the reactor to perform hydrogenation. The size of the obtained powder varied from 1 to 5 mm. The reactor containing the sample was evacuated to the pressure of 10^{-2} mmHg first at room temperature and then at 300°C for 30 min. The hydrogenation was performed at the set temperature. The amount and absorption rate of hydrogen were determined according to the change in pressure in the calibrated volume vessel.

The X-ray analysis of hydrogenation products was performed with a DRON-3 diffractometer (CuK_α radiation). The calculation of phase content in hydrogenation products was performed by profile refinement using Rietan2000 software.

After hydrogenation, the obtained powders were sifted through laboratory sieves with the cell sizes of 0.4 and 0.1 mm, respectively. The obtained 0.1–0.4 mm fraction was selected as the reactive one for the hydro-

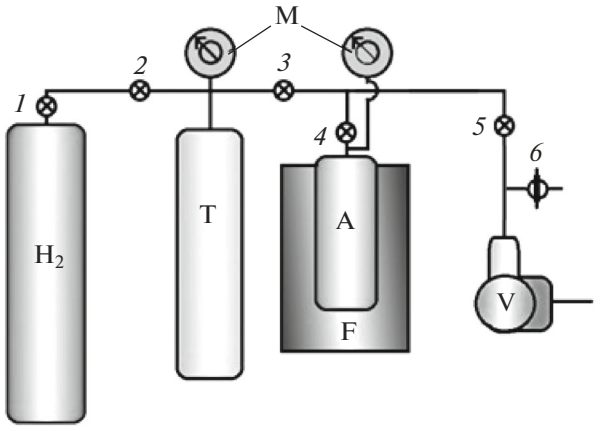

Fig. 1. Schematic of laboratory hydrogenation facility for the pressure range up to 100 bar: (*1–5*) valves; (A) reactor; (T) surge tank; (M) manometers; (V) vacuum station; (F) furnace; (*6*) glass valve.

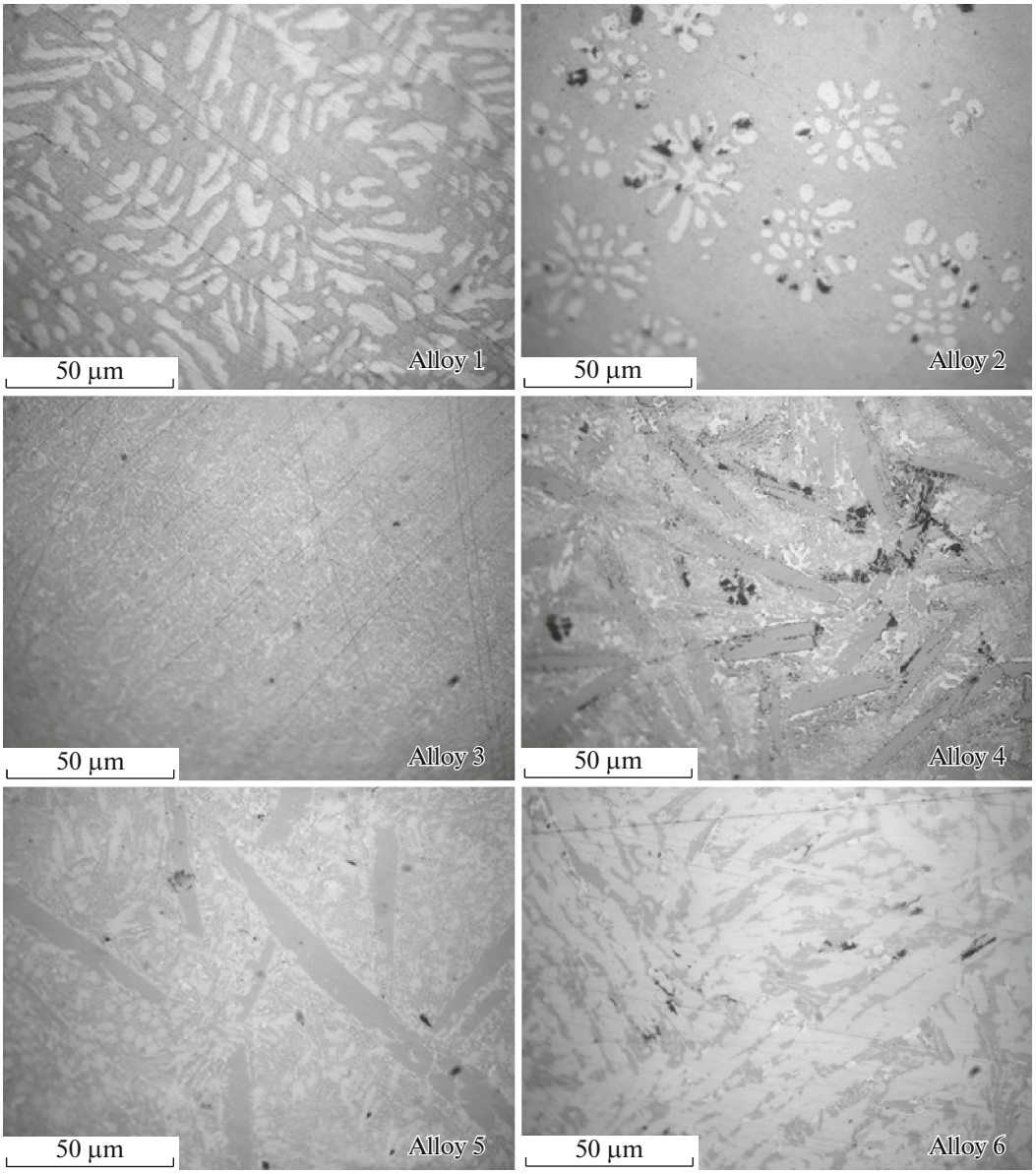

Fig. 2. Microstructure of alloys.

lysis. The amount of hydrogen generated during hydrolysis was measured using a Dwyer GFM2-H2 digital flowmeter calibrated against hydrogen. The reaction vessel was thermostated in a LOIP LT 105a thermostat; hydrolysis was performed in 10% wt NaCl solution at 25°C.

RESULTS AND DISCUSSION

Figure 2 depicts the microstructure of experimental alloys. The results of qualitative assessment of phase components according to the results of analysis of microstructure of alloys are given in Table 2. The data indicate that the alloys characterized by a chemical composition similar to the desired one were obtained by alloying.

Figure 3 shows the data on absorption time and amount of hydrogen absorbed by the studied alloys. It should be mentioned that hydrogenation of alloys was performed during a single cycle without preliminary activation of powders.

The experiments showed that alloys no. 5 and no. 6 exhibit the highest rate of hydrogen absorption, while two-component alloy no. 1 and three-component alloy no. 3 containing the lowest amount of rare-earth metals demonstrate the lowest hydrogenation rate.

The results of X-ray study of phase composition of hydrides are given in Table 3.

Table 2. Phase components of the samples of alloys according to microstructure analysis data

No.	Phase components
1	40% magnesium primary crystals 60% binary eutectic (Mg + Mg_2Ni)
2	8% magnesium primary crystals 92% binary eutectic (Mg + Mg_2Ni)
3	100% ternary eutectic (Mg + Mg_2Ni + $Mg_{12}Mm$)
4	53% Mg_2Ni primary crystals 47% ternary eutectic (Mg + Mg_2Ni + $Mg_{12}Mm$)
5	30% Mg_2Ni primary crystals 70% ternary eutectic (Mg + Mg_2Ni + $Mg_{12}Mm$)
6	65% $Mg_{12}Mm$ primary crystals 35% ternary eutectic (Mg + Mg_2Ni + $Mg_{12}Mm$)

The comparison of hydrogenation rate and phase composition of hydrides allows concluding that the increase in the amount of Mg_2Ni phase and the increase in the content of rare earth metals provide the increase in hydrogen absorption rate. The content of hydrogen in the alloys after 36 h of hydrogenation is presented in Table 4.

As mentioned above, the increase in concentration of rare earth metals in the alloy provides the increase in hydrogenation rate. On the other hand, the decrease in magnesium concentration leads to the decrease in total gravimetric hydrogen storage density because magnesium is the lightest component of the alloy. According to the results of the study, the increase in concentration of rare earth metals from 12.0 to 24.2% does not lead to a significant shortening of hydrogenation time. Therefore, the composition of alloy no. 5 is the optimal one in terms of the ratio between the hydrogenation time and the amount of absorbed gas.

The generalized results of hydrolysis of hydrogenated alloys are given in Fig. 4. The rate of hydrolysis weakly depends on the initial composition of the alloy; the total specific volume of hydrogen generated in 10 min varies from 924 to 1184 mL/g. The rate of hydrogen release during hydrolysis is maximal at the initial moment of time; it decreases during the reaction because of the formation of a passivating layer of magnesium hydroxide on the surface of hydride particles. The results of estimation of conversion after 10 min of the reaction with aqueous solution of magnesium chloride are given in Table 5.

CONCLUSIONS

A comprehensive study of the influence of the doping elements on the rate of hydrogen absorption by magnesium alloys and hydrogen generation during hydrolysis of hydrogenated alloys was performed. The positive influence of Ni and rare earth doping ele-

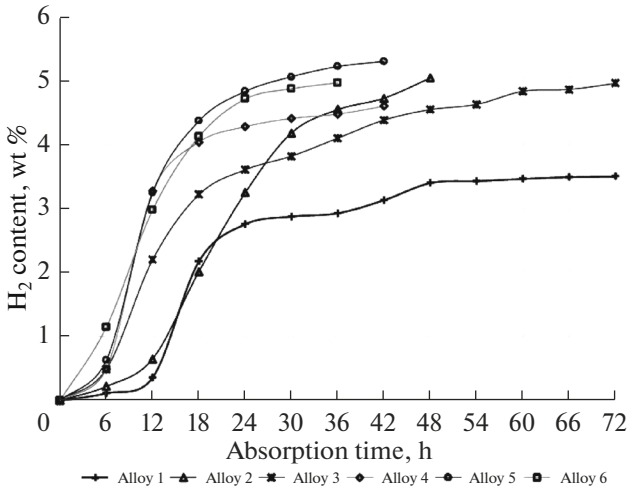

Fig. 3. Curves of hydrogen absorption by alloys.

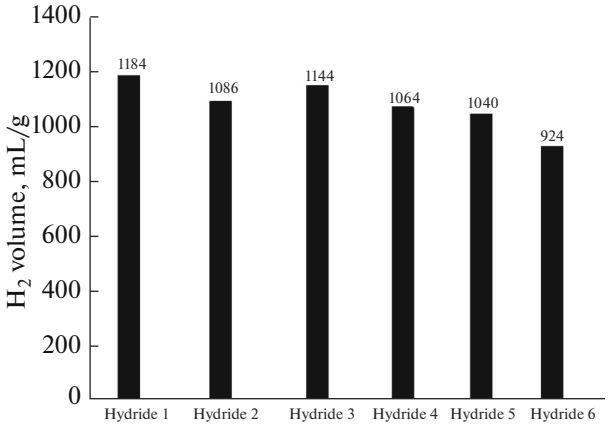

Fig. 4. Results of hydrogen generation by hydrolysis of alloy hydrides (hydrolysis was performed for 10 min at 10°C).

Table 3. Phase composition of alloy hydrides according to the X-ray analysis data (wt %)

Alloy no.	MgH_2	Mg_2NiH_4	MmH_3
1	44.4	26.9	28.7
2	62.2	32.9	4.9
3	54.1	25.2	20.7
4	76.6	23.4	–
5	48.4	51.6	–
6	63.7	31.2	5.1
7	58.1	34.6	7.3

Table 4. Amount of hydrogen absorbed by alloys in 36 h

Alloy no.	H_2 content, wt %
5	5.2
6	5.0
2	4.5
4	4.5
3	4.1
1	2.9

Table 5. Conversion at hydrolysis of alloy hydrides in 10 min

Alloy no.	Theoretical volume of hydrogen, mL/g	Experimental volume of hydrogen, mL/g	Conversion, %
1	1108	970	87.5
2	1348	1132	84.0
3	1222	1176	96.2
4	1493	1200	80.3
5	1241	1216	98.0
6	1361	1207	88.7
7	1303	1067	81.8

ments on the hydrogen absorption rate was estimated. The optimal concentration of rare earth metals in the alloy equal to 12 wt % was determined. The highest amount of hydrogen (5.2 wt %) was absorbed by the alloy of $MgNi_{25}Mm_{12}$ composition. This alloy is characterized by the maximum conversion (98%) after 10 min of hydrolysis reaction.

FUNDING

This work was supported by the Foundation for Innovations Assistance (project no. 2104GS1/35284, 31.08.2017).

REFERENCES

1. Ferreira, H., Garde, R., Fulli, G., Kling, W., and Lopes, J., Characterization of electrical energy storage technologies, *Energy*, 2013, vol. 53, pp. 288–298.
2. Varin, R.A., *Nanomaterials for Solid State Hydrogen Storage*, New York: Springer-Verlag, 2009.
3. Kim, J. and Kim, T., Compact PEM fuel cell system combined with allin-one hydrogen generator using chemical hydride as a hydrogen source, *Appl. Energy*, 2015, vol. 160, pp. 945–953.
4. Kim, S.J., Hydrogen generation system using sodium borohydride for operation of a 400W-scale polymer electrolyte fuel cell stack, *J. Power Sources*, 2007, vol. 170, pp. 412–418.
5. Sim, J., Hydrogen generation from solid-state $NaBH_4$ particles using $NaHCO_3$ agents for PEM fuel cell systems, *Energy Procedia*, 2014, vol. 61, pp. 2058–2061.
6. Yang, L., Guo, J., Huang, W.C., and Jang, B.Z., US Patent 20060112635, 2006.
7. Stepan, C.R., Adams, P., Curello, A.J., Sgroi, A., and Fairbanks, F., US Patent 20080206113, 2008.
8. Cenci, G., Vizza, F., Filippi, J., Marchionni, A., and Bianchini, C., EU Patent 2013021243, 2013.
9. Amendola, S.C., Petillo, P.J., Petillo, S.C., and Mohring, R.M., US Patent 6932847, 2005.
10. Wang, H., The hydrolysis behavior of Mg_2Ni and Mg_2NiH_4 in water or a 6 M KOH solution and its application to Ni nanoparticles synthesis, *J. Alloys Comd.*, 2009, vol. 470, pp. 539–543.
11. Tegel, M., Schöne, S., Kieback, B., and Röntzsch, L., An efficient hydrolysis of MgH_2-based materials, *Int. J. Hydrogen Energy,* 2017, vol. 42, pp. 2167–2176.
12. Ouyang, L., Enhanced hydrogen generation properties of MgH_2-based hydrides by breaking the magnesium hydroxide passivation layer, *Energies*, 2015, vol. 8, pp. 4237–4252.
13. Hiraki, T., Hiroi, S., Akashi, T., Okinaka, N., and Akiyama, T., Chemical equilibrium analysis for hydrolysis of magnesium hydride to generate hydrogen, *Int. J. Hydrogen Energy*, 2012, vol. 37, pp. 12114–12119.
14. Klyamkin, S.N., Verbetskii, V.N., and Semenenko, K.N., Hydrogenation of magnesium in the presence of hydride of rare earth metals, *Izv. Akad. Nauk SSSR, Met.*, 1989, no. 2, pp. 182–187.
15. Kuliev, S.I., Klyamkin, S.N., Verbetskii, V.N., Gasanzade, A.A., and Semenenko, K.N., Interaction of alloys magnesium–mischmetal–nickel with hydrogen, *Izv. Akad. Nauk SSSR, Met.*, 1988, no. 1, pp. 173–176.
16. Huang, J.M., Ouyang, L.Z., Wen, Y.J., Wang, H., Liu, J.W., Chen, Z.L., and Zhu, M., Improved hydrolysis properties of Mg_3RE hydrides alloyed with Ni, *Int. J. Hydrogen Energy*, 2014, vol. 39, pp. 6813–6818.
17. Semenenko, K.N., Verbetskii, V.N., Mitrokhin, S.V., and Burnasheva, V.V., The interaction of intermetallic compounds of zirconium crystallized in structural types of Laves phases with hydrogen, *Zh. Inorg. Khim.*, 1980, no. 7, pp. 1731–1736.

Translated by P. Vlasov